Thin-Walled Structures 48 (2010) 482–494

Contents lists available at ScienceDirect

Thin-Walled Structures

journal homepage: www.elsevier.com/locate/tws

Partial Al foam filling of commercial 1050H14 Al crash boxes: The effect of box column thickness and foam relative density on energy absorption

A.K. Toksoy [a,b], M. Güden [a,b,*]

[a] Dynamic Testing and Modeling Laboratory, Izmir Institute of Technology, Gulbahce Koyu, Urla, Izmir, Turkey
[b] Department of Mechanical Engineering, Izmir Institute of Technology, Gulbahce Koyu, Urla, Izmir 35430, Turkey

ARTICLE INFO

Article history:
Received 1 December 2009
Received in revised form
4 February 2010
Accepted 4 February 2010
Available online 18 February 2010

Keywords:
Crash box
Simulation
Al foam
Crushing
Energy absorption

ABSTRACT

The crushing behavior of partially Al closed-cell foam filled commercial 1050H14 Al crash boxes was determined at quasi-static and dynamic deformation velocities. The quasi-static and dynamic crushing of the boxes were simulated using the LS-DYNA. The results showed that partial foam filling tended to change the deformation mode of empty boxes from a non-sequential to a sequential folding mode. In general, the experimental and simulation results showed similar mean load values and deformation modes. The SEA values of empty, partially and fully foam filled boxes were predicted as function of box wall thickness between 1 and 3 mm and foam filler relative density between 0 and 0.2, using the analytical equations developed for the mean crushing loads. The analysis indicated that both fully and partially foam filled boxes were energetically more efficient than empty boxes above a critical foam filler relative density. Partial foam filling, however, decreases the critical foam filler density at increasing box wall thicknesses.

1. Introduction

Constructed generally in tubular form of ductile metals including steel and Al, crash boxes are the passive safety systems preventing the excessive deformation of the automobile chassis against the frontal crashes. Tubular structures, as is known, deform progressively under compressive loads by a wall folding mechanism that usually results in relatively high specific energy absorption (SEA) and energy absorption efficiency. The crushing behaviors of tubular structures have been subjected to extensive experimental and numerical investigations for the last several decades. Various geometries including cylindrical [1–3], square [4–6] and hexagonal [7,8] cross-sections, multi-cell structures [9,10] and light-weight foam filling [11–15] have been investigated for improving the crushing behavior of tubular structures under quasi-static and dynamic loads. Particularly, the light-weight Al closed-cell foam filling has been taken considerable interest recently, as relatively cheaper Al closed-cell foams are produced by several companies using various foaming methods. On a large production scale, it is further expected that the relatively high prices of Al foams would decline significantly.

In foam filled tubular structures, an interaction effect between foam filler and tube wall was usually noted and resulted in tube crushing loads higher than the sum of the crushing load of empty tube alone and foam filler alone [11,12,16]. The interaction effect in square cross-section tubes was however found higher than in circular tubes, while foam filled circular tubes exhibited higher SEA values on the same weight basis [17]. Various material and geometrical parameters were shown to affect the SEA in foam filled tubes. Increase in foam filler density and the tube wall thickness generally increased the SEA values [5]. It was also shown that foam filling resulted in energetically efficient structures when the filler density was above a critical value, signifying the effect of foam filler density on the energy absorption characteristics of the filled tube [16]. The deformation of the foam filler in the filled tubes was further considered composing of a densified region in the mid-sections of the deformed foam filler and an extremely densified region near the tube wall [14]. The interaction effect was attributed to the formation of the extremely densified region near the tube wall. An appropriate foam filler length in partially foam-filled columns (the foam filler length is smaller than the column length) was shown to provide energetically more efficient structures, in addition to a lower initial peak force than the fully foam-filled columns [18]. The present report is a part of an on-going experimental and numerical research program on the effect of material and geometrical parameters on the energy absorption behavior of partially Al foam filled commercial 1050H14 Al

* Corresponding author at: Department of Mechanical Engineering, Izmir Institute of Technology, Gulbahce Koyu, Urla, Izmir 35430, Turkey.
Tel.: +90 232 7506779; fax: +90 232 7506701.
E-mail address: mustafaguden@iyte.edu.tr (M. Güden).

0263-8231/$ - see front matter © 2010 Elsevier Ltd. All rights reserved.
doi:10.1016/j.tws.2010.02.002

Table 1
1050H14 Al alloy tensile properties.

Direction	Young's modulus E (GPa)	Tangent modulus E_t (MPa)	Yield strength $\sigma_{0.2}$ (MPa)	Ultimate tensile strength σ_u (MPa)	Poison ratio v	Failure strain (%)
Parallel to extrusion direction	70	147	105	110	0.33	8.4

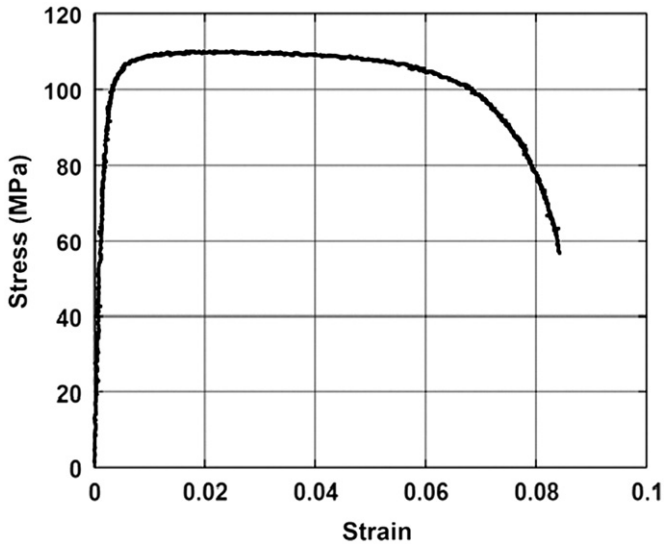

Fig. 1. Typical engineering stress–strain curve of a 1050H14 Al alloy at $2.77 \times 10^{-3}\,s^{-1}$.

automobile crash boxes and focuses on the effects of crash box thickness and foam filler density on the energy absorption of partial foam filling, which has not been investigated, yet. The quasi-static and dynamic crushing of filled and empty crash boxes in two different cross-sections and three different thicknesses were simulated using the LS-DYNA. The efficiency of energy absorption of partially foam filled boxes was finally assessed in comparison with that of empty and fully foam filled boxes.

2. Materials and testing

The mechanical properties of 1050H4 Al sheet alloy determined through tensile testing in accord with ASTM E8 standard [19] are tabulated in Table 1. The typical engineering stress–strain curve of the alloy at a strain rate of $2.77 \times 10^{-3}\,s^{-1}$ is shown in Fig. 1. The alloy has an average 0.2% proof strength of 105 MPa and a failure strain of 8.4%. The relative density (ρ^*—density of foam/density of aluminum) of as-received Alulight AlSi10 closed-cell foam panels ($625 \times 625 \times 30$ mm) ranged between 0.11 and 0.215. Uniaxial compression tests were performed at a crosshead speed of $5\,mm\,min^{-1}$ ($1.6 \times 10^{-3}\,s^{-1}$) on the cubic foam samples ($30 \times 30 \times 30$ mm) through the panel thickness direction. Fig. 2a shows the compression stress–strain curves of Al foam filler at various relative densities. The plateau stress (σ_f) is determined by simply averaging the stress values between the initial collapse and 0.1 strain (shown by box in Fig. 2a). The determined experimental plateau stress values are then fitted with a power law strengthening equation as (Fig. 2b),

$$\sigma_p = A(\rho^*)^n \tag{1}$$

where, A and n are the constants. The values of A and n are found to be 494.08 MPa and 2.963, respectively. The foams with 0.11

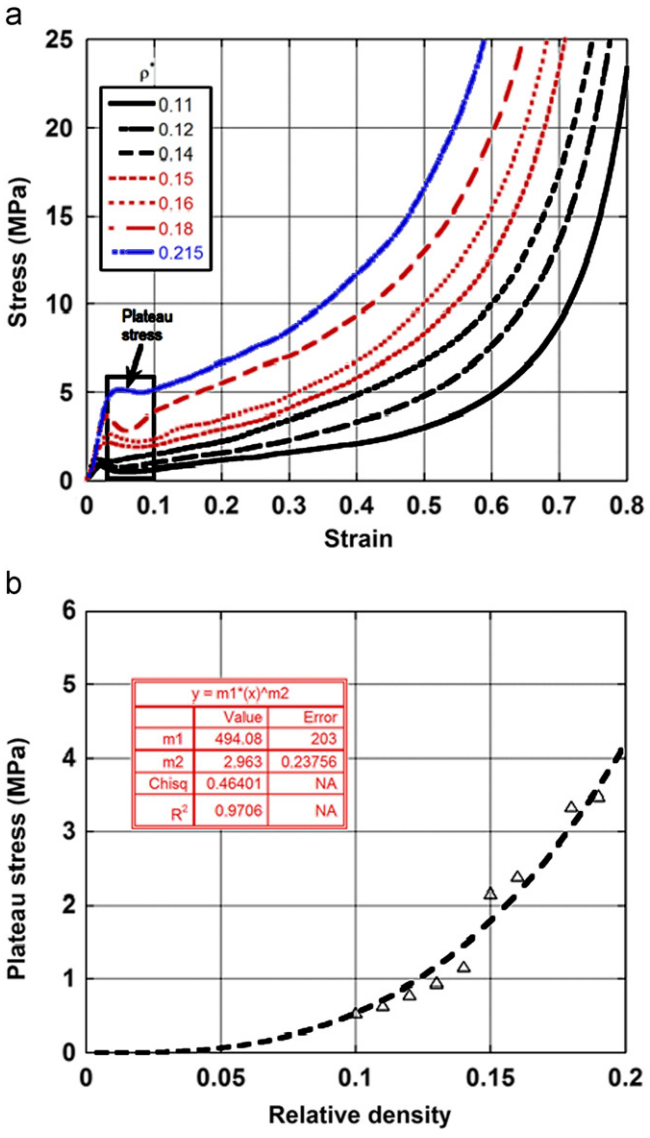

Fig. 2. (a) Compression stress–strain curves of the Alulight AlSi10 foam and (b) plateau stress vs. relative density.

($297\,kg\,m^{-3}$) and 0.15 ($405\,kg\,m^{-3}$) relative densities were used to fill Al crash boxes for compression testing. The plateau stresses of the foam at 0.11 and 0.15 relative densities are determined to be 0.65 and 2.17 MPa, respectively.

As-received commercial Al crash boxes in two different sizes ($73 \times 70 \times 120$ and $70 \times 60 \times 120$ mm) were manufactured by a series of processing routes including laser cutting, bending and TIG welding of 1050H14 Al sheets. Four V-shaped grooves were formed on the opposite surfaces of the boxes, two near the top and two near the bottom of the boxes as depicted in Fig. 3a. The distance between each V-groove on the same face of the boxes

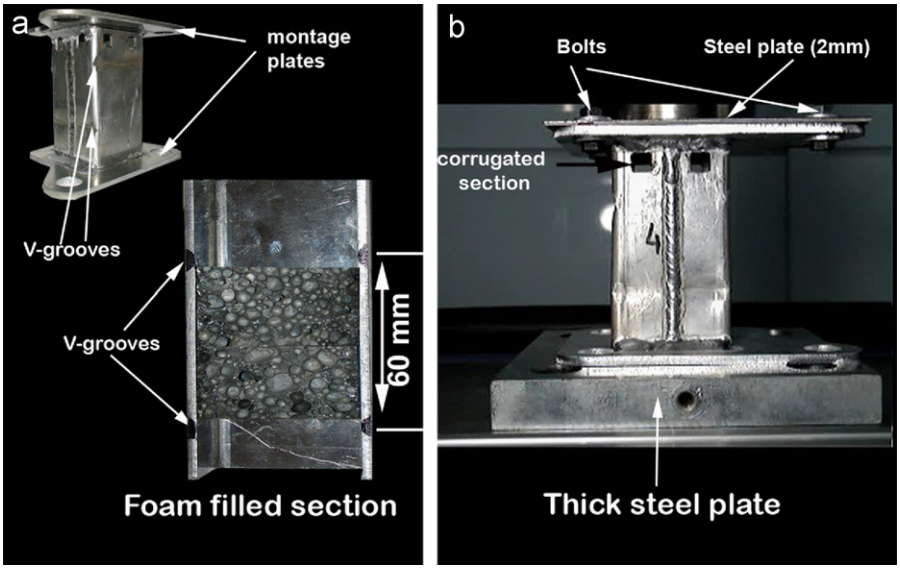

Fig. 3. (a) The cross-section of a partially foam filled 3 mm thick G1 box showing V-grooves on the surface and (b) the picture of a foam filled crash box in compression testing.

Table 2
Test samples and coding.

Geometry	Box wall thickness (t)	Filling	Coding
G1	2	E	G1T2E
G1	2	F1	G1T2F1
G1	2	F2	G1T2F1
G1	2.5	E	G1T2.5E
G1	2.5	F1	G1T2.5F1
G1	2.5	F2	G1T2.5F2
G1	3	E	G1T3E
G1	3	F1	G1T3F1
G1	3	F2	G1T3F2
G2	2	E	G2T2E
G2	2	F1	G2T2F1
G2	2	F2	G2T2F2
G2	2.5	E	G2T2.5E
G2	2.5	F1	G2T2.5F1
G2	2.5	F2	G2T2.5F2
G2	3	E	G2T3E
G2	3	F1	G2T3F1
G2	3	F2	G2T3F2

G1: $73 \times 70 \times 120$ mm box; G2: $70 \times 60 \times 120$ mm box; E: empty; F1: foam filled (relative density 0.11); F2: foam filled (relative density 0.15).

was 60 mm. Two layers of foam filler (each 30 mm in thickness) were inserted in between the grooves. As the foam layers were tightly held between the grooves, no bonding agent use was required between the layers of foam fillers and also between foam filler and box wall. The grooves also fixed the foam filler at the middle of the box during compression testing. At the top of the boxes, a corrugated section (two square holes on each face) was intentionally machined in order to form an easy fold initiation site (Fig. 3b). The compression tests were performed by means of the montage plates welded at the ends of the box (Fig. 3a). The montage plates were made from the same alloy sheet of the crash boxes, 1050H14 Al, with a thickness of 5 mm. Table 2 tabulates the coding used to test empty and filled boxes. In the table, G1 and G2 refer to the boxes in $73 \times 70 \times 120$ and $70 \times 60 \times 120$ mm size, respectively.

Quasi-static tests on empty and partially Al foam filled boxes were performed using a Schmadzu AGI 300 kN universal testing machine. The boxes were compression tested between two rigid steel plates as shown in Fig. 3b. The top steel plate, 2 mm in thickness, was fastened to the upper montage plate with the bolts. The compression tests were performed at a displacement rate of 500 mm min^{-1}, corresponding to a strain rate of 6.6×10^{-2} s^{-1}. In order to determine the effect of impact velocity on the crushing load of empty and filled boxes, several empty and F1 foam filled 3 mm thick G1 boxes were dynamically compression tested using a Fractovis Plus drop-weight test system at a velocity of 5.5 m s^{-1}. The dynamically tested boxes were sequentially reloaded (three times) at the same impact speed in order to reach relatively high displacements.

3. Model description

The details of filled box model are shown in Figs. 4a and b. The 1050H4 Al crash box was modeled using 4 node Belytschko–Tsay shell elements, one point integration in the plane and five in the thickness direction. The foam filler was modeled using 8-node solid elements and the top and bottom montage plates using shell elements. In the model, the translation and rotation of the bottom montage plate were restricted and the weldments between montage plates and crash box were simulated by nodal constraints. The width of the welding zone was measured 6 mm; therefore, the rotational motions of the nodes at a distance of 6 mm from the top and bottom of the crush boxes were restricted in all directions (Fig. 4a). The translation motion of the welding zone nodes was only allowed in the long axis of the box. Similar constraints were also previously applied in the simulation of the crushing of a 5018 Al tube [20]. The self contacting crush zone surfaces (folds) were modeled using automatic single surface contact algorithm in the LS-DYNA (Fig. 4b). The contacts between foam and box and between foam and montage plates were modeled using automatic surface to surface contact (Fig. 4b). The contact between box and montage plate was modeled with automatic nodes to surface contact algorithm (Fig. 4b). The static and dynamic friction coefficients were taken to be 0.3 and 0.2, respectively.

The box and montage plate material, 1050H14 Al, were modeled using plastic kinematic material model (Mat 3). In plastic kinematic material model, the mechanical properties are characterized by the material yield strength (σ_o), the Young's modulus (E) and the tangent modulus (E_t: the slope of the

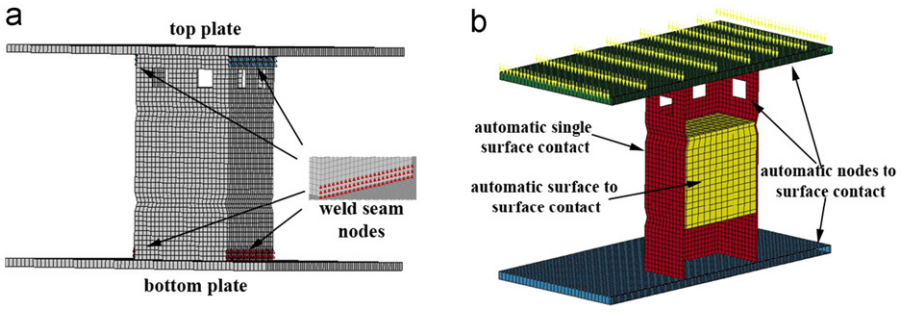

Fig. 4. The details of foam filled crash box model; (a) overall view and (b) cross-sectional view.

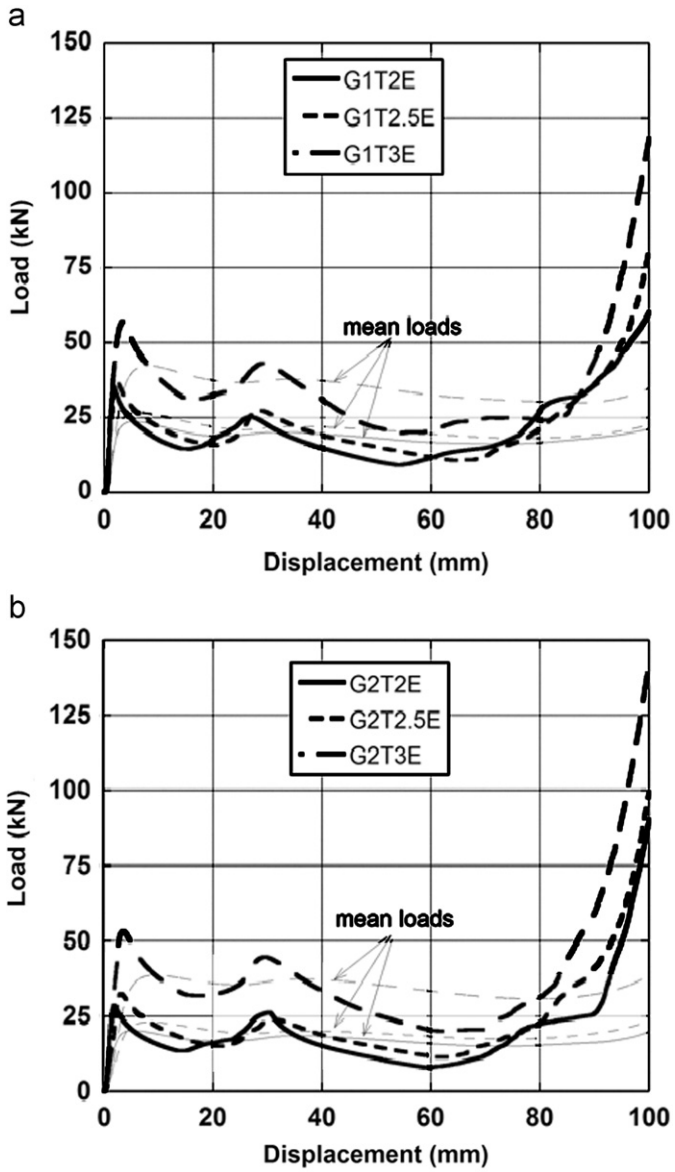

Fig. 5. Experimental load and mean load-displacements curves of (a) G1 and (b) G2 empty boxes.

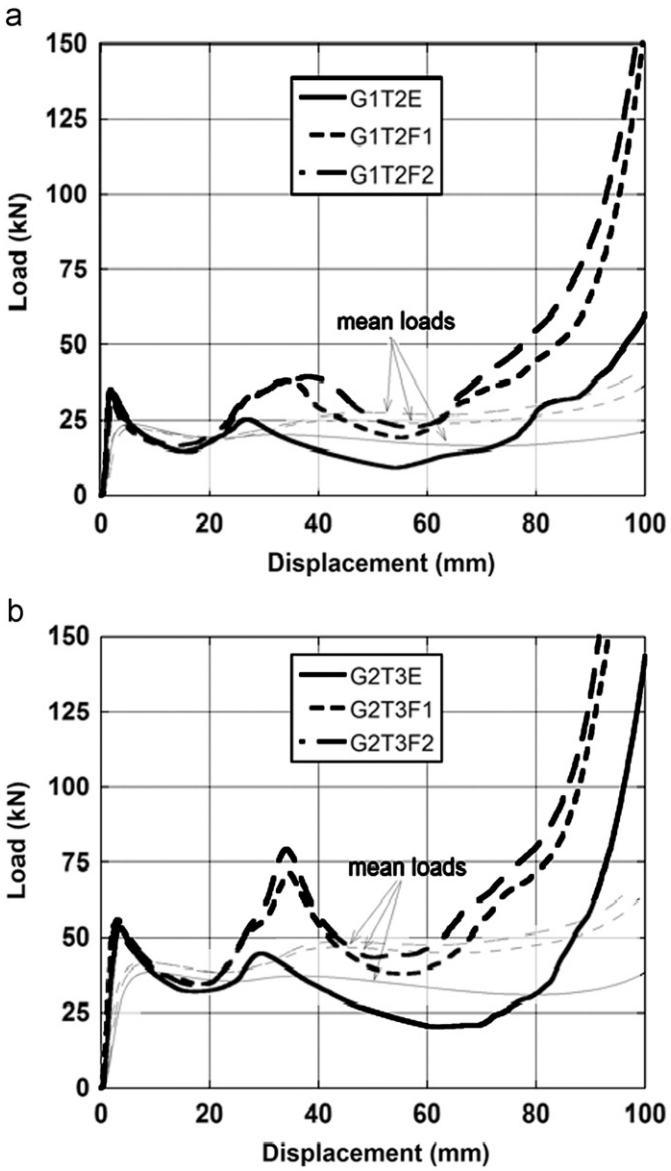

Fig. 6. Experimental load and mean load-displacement curves of empty and foam filled boxes: (a) 2 mm thick G1 boxes and (b) 3 mm thick G2 boxes.

stress–strain curve in the plastic region). The yielding is defined by von Mises yield criterion. In plastic kinematic plasticity algorithm, the flow stress (σ) is given as

$$\sigma = \sigma_o + \beta E_p \varepsilon_{\text{eff}}^p \tag{2}$$

where, β is the hardening coefficient and $\varepsilon_{\text{eff}}^p$ and E_p are the effective plastic strain and plastic hardening modulus, respectively. The plastic hardening modulus is calculated using the

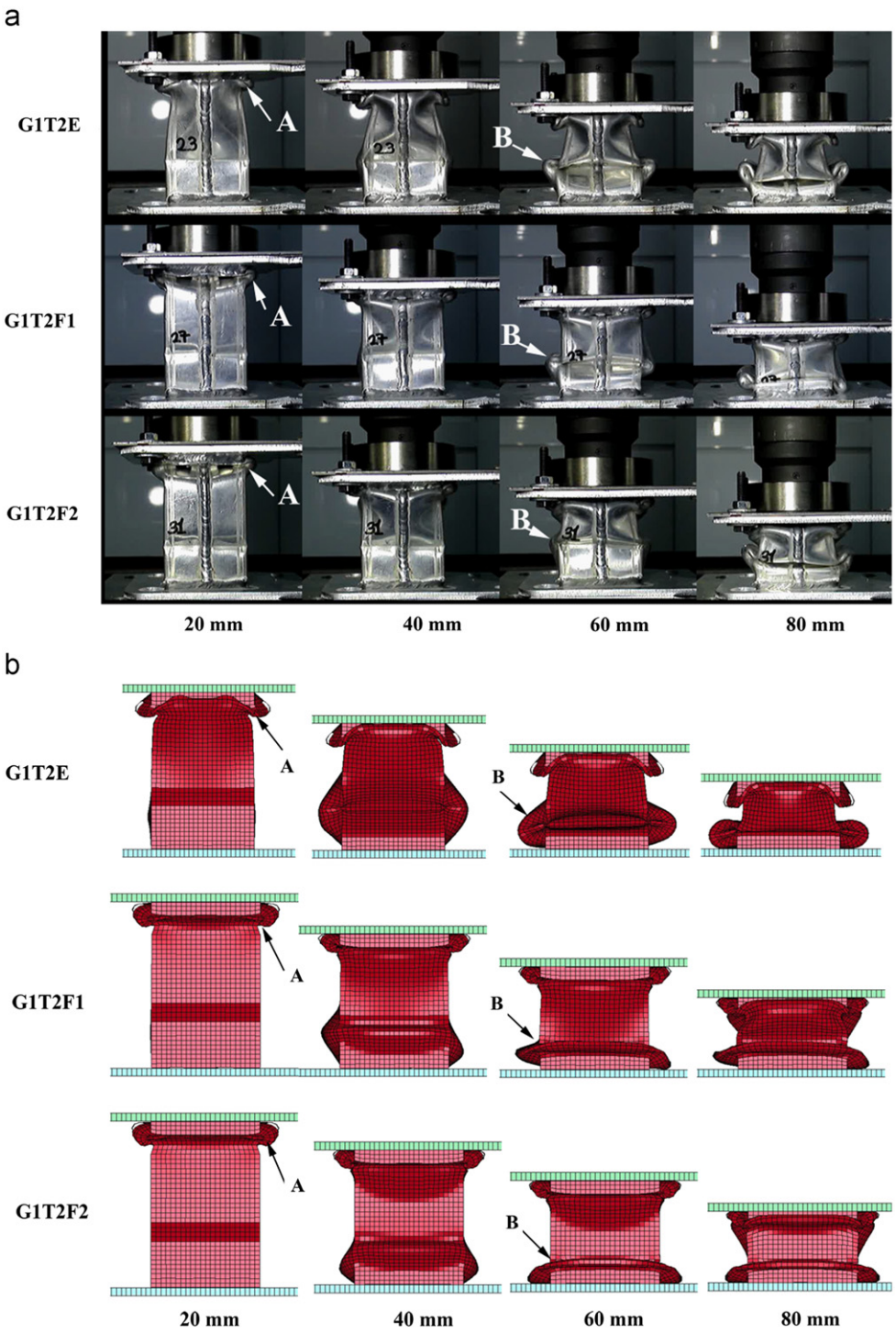

Fig. 7. (a) Experimental and (b) simulation deformation pictures of 2 mm thick empty and filled G1 boxes.

following relation

$$E_p = \frac{EE_t}{E-E_t} \tag{3}$$

Al foam filler was modeled using honeycomb material model (Mat 26). Honeycomb material model is essentially anisotropic when considered in axial and transverse directions; therefore, the material parameters are required to be determined separately for each direction. Al foams are usually considered nearly isotropic, showing small variations in mechanical properties in 3 directions; therefore, the mechanical properties in three directions are considered to be the same [16]. The material model further assumes that the foam behaves as a solid and switches to an isotropic elastic perfectly plastic material with von Mises yield criterion after densification strain. Thus, densification strain of foam material should be described for Al foam modeling using the Mat 26.

The quasi-static crushing simulations in the LS-DYNA require mass scaling. Two methodologies of mass scaling are generally applied [21]: scaling down the material density (the total time of

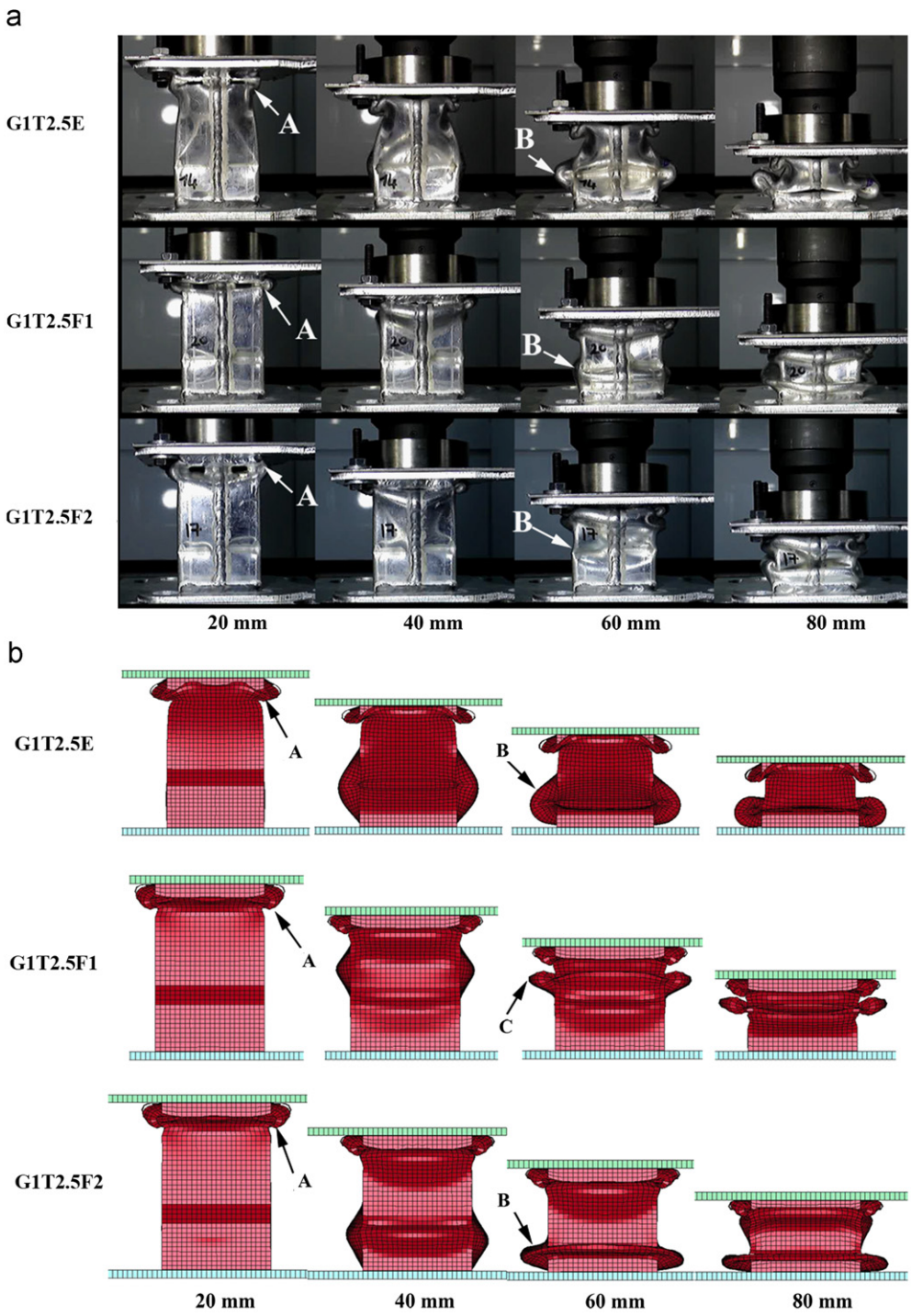

Fig. 8. (a) Experimental and (b) simulation deformation pictures of 2.5 mm thick empty and filled G1 boxes.

solution is decreased by increasing the loading rate of quasi-static simulation) and scaling up the mass density at very low loading rates (very large time steps). In quasi-static simulation using mass scaling, two conditions must be satisfied. The total kinetic energy must be very small compared to total internal energy and the load-displacement curves must be independent of the deformation rate. Above conditions were found to be satisfied in the quasi-static simulations of the empty and filled boxes by scaling down the material mass density by a factor of 1000 at $2\,m\,s^{-1}$ deformation rate. In the simulations of the dynamic crushing tests, the velocity of the top compression plate was $5.5\,m\,s^{-1}$.

4. Results and discussions

The effect of box column thickness on the load and mean load values of G1 and G2 empty boxes is shown in Figs. 5a and b, respectively. As the box thickness increases, both the load and mean load values of the boxes increase. The effect of foam filling on the load and mean load values of 2 mm thick G1 and 3 mm thick G2 box is further shown in Figs. 6a and b, respectively. Partial foam filling, as seen in these figures, becomes effective above 10–20 mm displacement; thereafter, the load and mean load values of filled boxes increase over those of empty boxes,

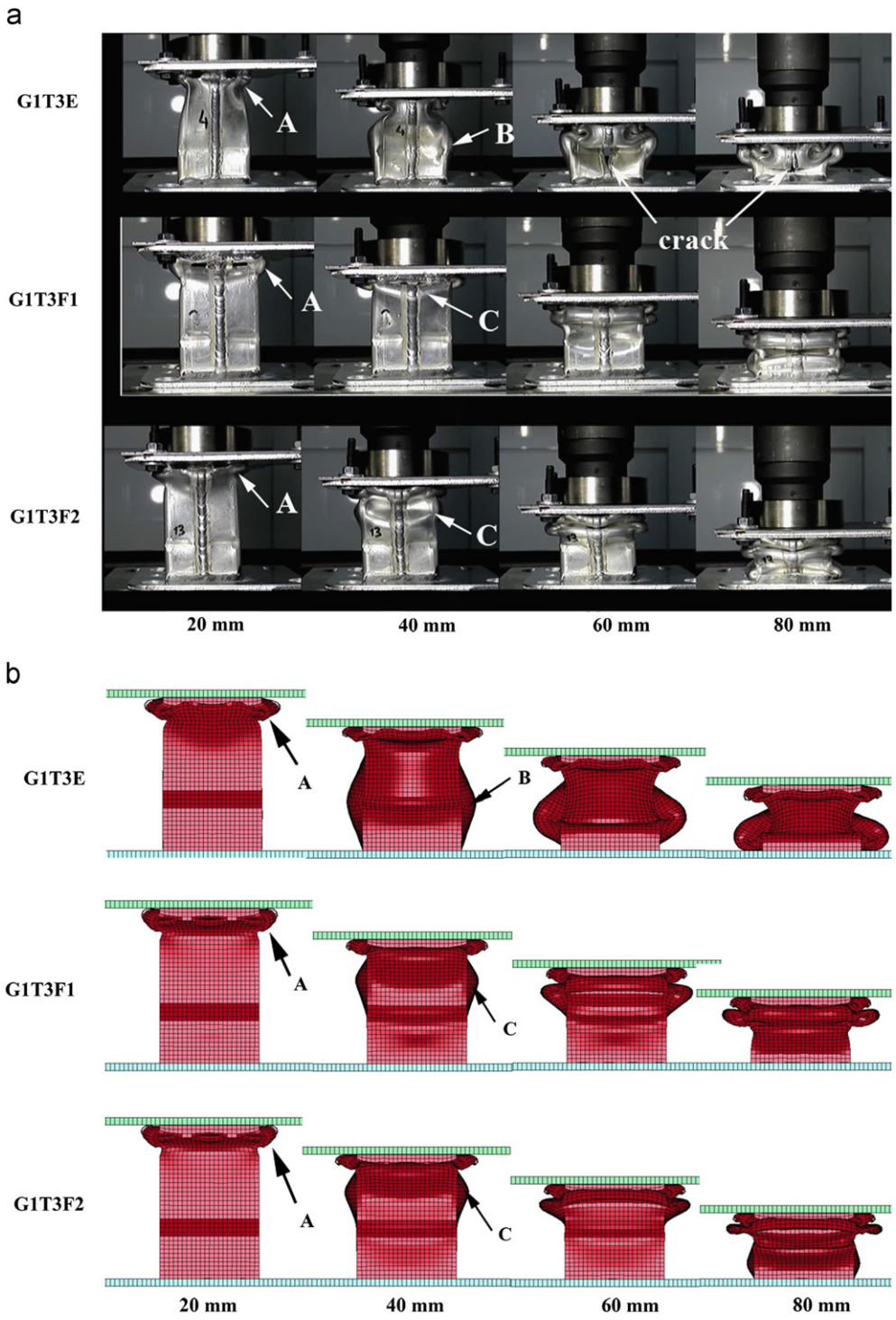

Fig. 9. (a) Experimental and (b) simulation deformation pictures of 3 mm thick empty and filled G1 boxes.

while higher relative density foam filling results in higher load and mean load values in all filled crash boxes tested.

The experimental and simulation deformation pictures of 2 mm thick empty and filled G1 boxes are sequentially shown in Figs. 7a and b. The folding begins, both experimentally and numerically, from the corrugated section (A in Figs. 7a and b). However, the folding is considered non-sequential (progressive folding at two different locations), since the following folds trigger both at the top V-grooves and bottom V-grooves (marked with B in Figs. 7a and b). A similar deformation mode is also observed experimentally in 2.5 mm thick empty and filled G1 boxes, depicted in Fig. 8a, while simulated F1 foam filled G1 box folding triggers at one of the of the top V-grooves (Fig. 8b). Three millimeter thick empty G1 box deforms experimentally and numerically in non-sequential mode, the same as 2 and 2.5 mm thick empty and filled G1 boxes, while the foam filled 3 mm thick G1 box deforms in sequential mode. The following second fold marked with C in Figs. 9a and b is initiated at one of the top V-grooves. Two and 2.5 mm thick empty and foam filled G2 boxes also showed non-sequential folding both numerically and

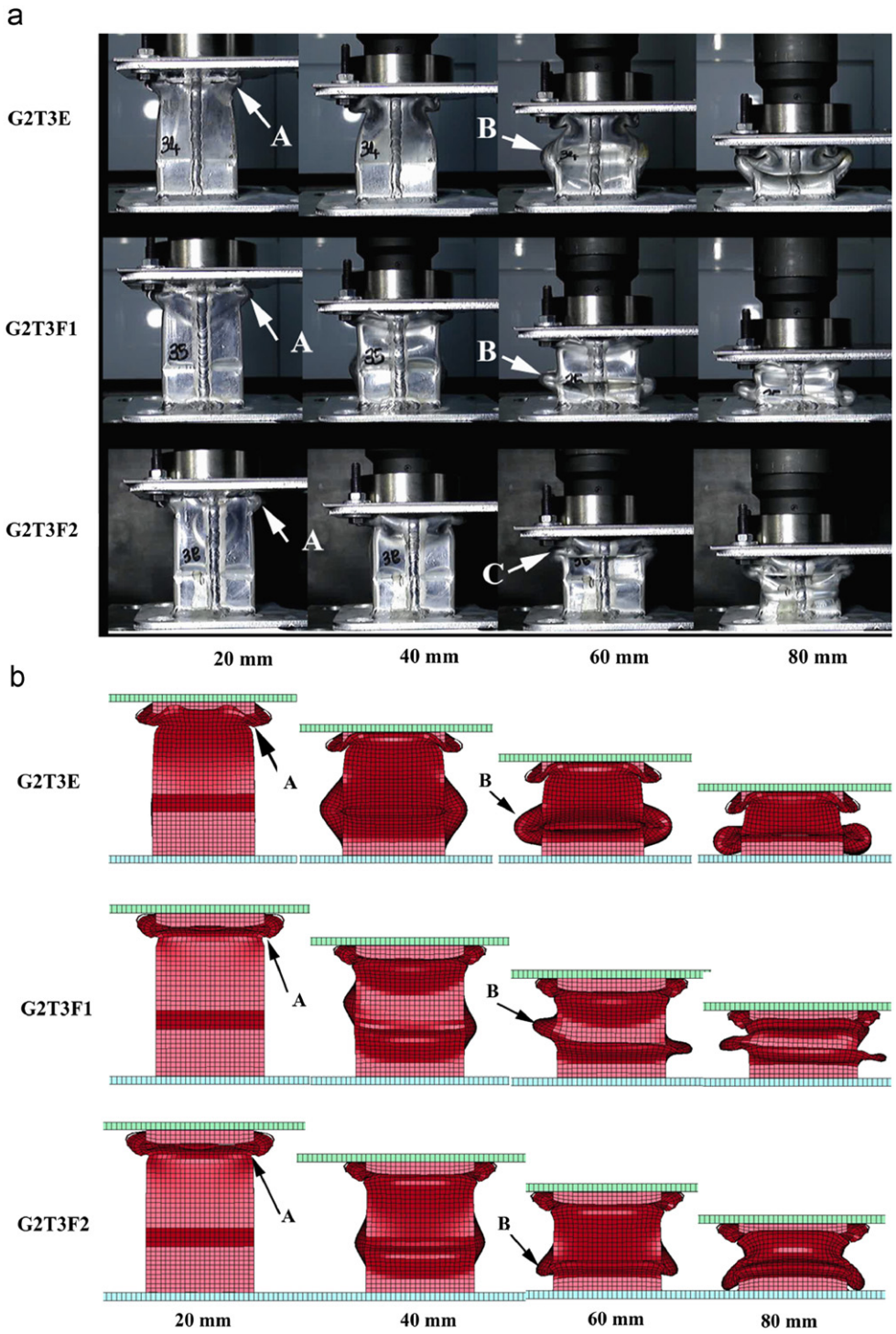

Fig. 10. (a) Experimental and (b) simulation deformation pictures of 3 mm thick empty and filled G2 boxes.

experimentally (not shown), similar to 2 and 2.5 mm thick empty and filled G1 boxes. The box column deformation in 3 mm thick empty and 0.1 relative density foam filled G2 box is however non-sequential as seen in Figs. 10a and b (marked with B), while it experimentally turns into a sequential folding mode in 0.15 relative density foam filled G2 box. Shortly, the bottom V-grooved section in empty boxes provides another easy folding side following the crushing of the corrugated section.

The weldments of the boxes are noted mostly intact during compression. In few crushed boxes, cracks extending in several millimeters in the weld section are seen (Fig. 9a); however, no significant effect of cracks is found on the load-displacement curves of the boxes. In empty G1 and G2 boxes, totally two folds form both experimentally and numerically, while foam filling increases the number of folds to 3. The effect of foam filling on the folding of the crash boxes is clearly seen in Fig. 11, in which empty and foam filled G1 boxes cross-sections (80 mm displacement) are shown together. As is seen in Fig. 11, the foam filling induces a shorter fold length by restraining inward folding of the box wall.

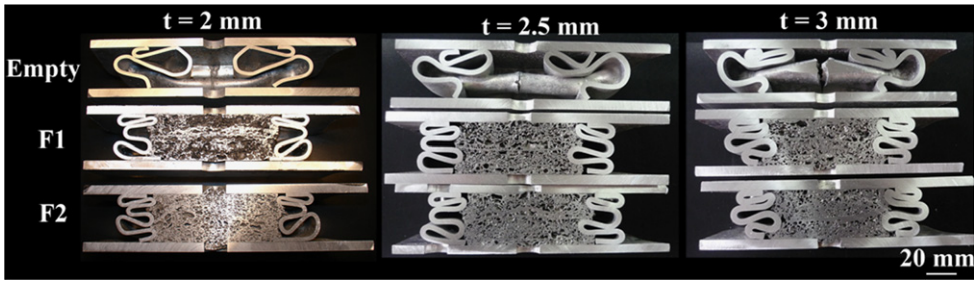

Fig. 11. Cross-section pictures of the compressed (80 mm) empty and foam filled G1 boxes.

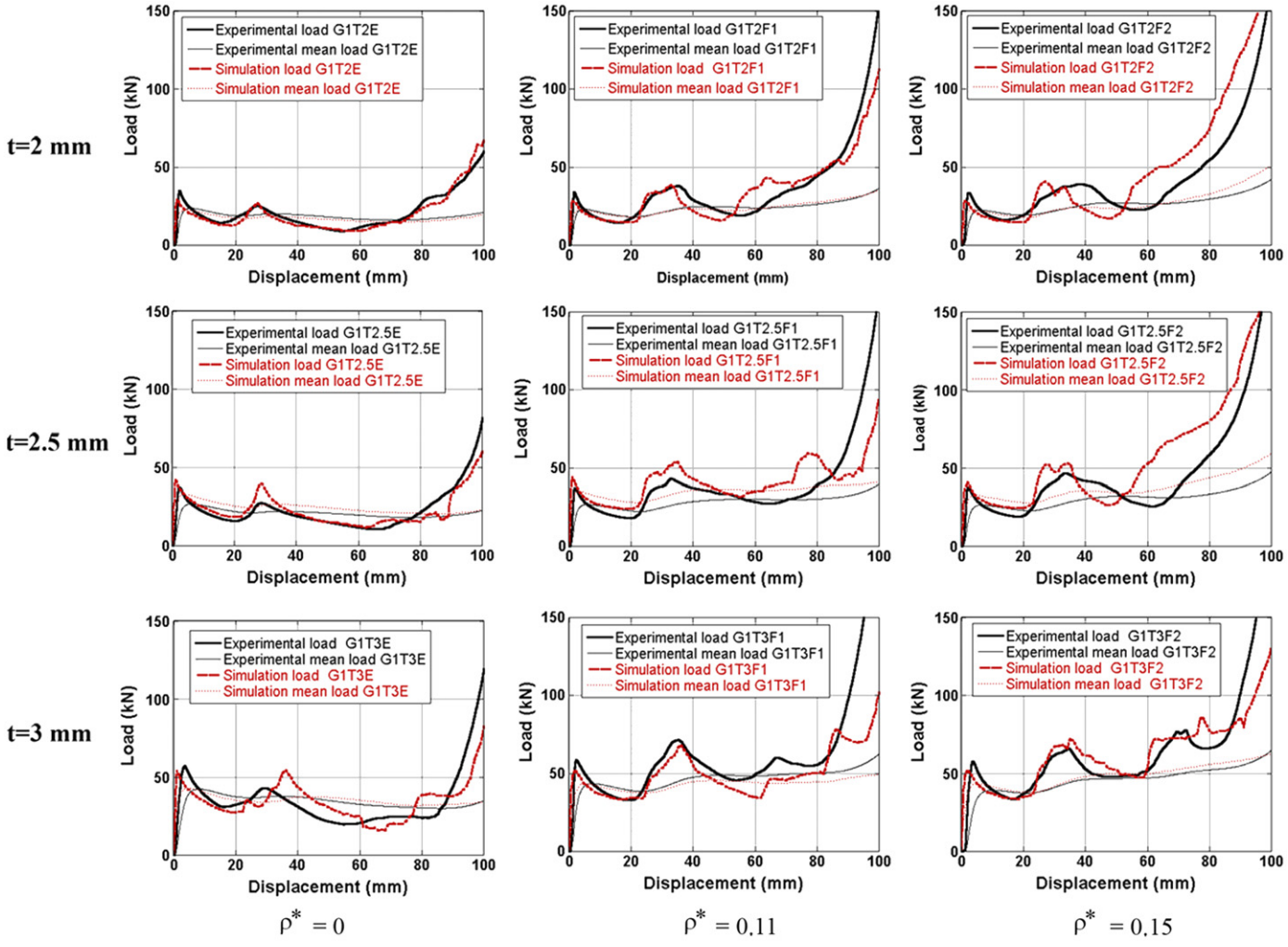

Fig. 12. Experimental and simulation load and mean load-displacement curves of G1 boxes as a function of box wall thickness and foam filler relative density.

The experimental and simulation load and mean load-displacement curves of empty and filled G1 boxes are shown in Fig. 12 as function of box wall thickness and foam filler density. Deformation load levels of the simulations generally show good agreements with those of experiments in 2 and 3 mm thick boxes, while the simulation mean load values are slightly higher than experimental values in both 2.5 mm thick G1 and G2 boxes. The dynamic reloading load and mean load-displacement curves of empty 3 mm thick G1crash box are shown in Fig. 13a together with static load and mean load-displacement curves for comparison. An initial peak load was seen at the beginning of load-displacement curve of each reloading test in dynamic load-displacement curve. This initial peak load region was excluded from the load-displacement curve except that of the first loading. As is seen in Fig. 13a, the load and mean load values of dynamically and quasi-statically tested boxes are almost the same in empty 3 mm thick G1 box. Fig. 13b shows simulation and experimental load and mean load-displacement curve of 3 mm thick F1 foam filled G1 box. Simulation and experimental load levels of filled G1 box are very similar to each other, although the second peak load is slightly shifted to larger deformations in the simulated curve. The deformation patterns of dynamically and quasi-statically tested empty and partially filled G1 box were also found to be very similar. It may be concluded that increase in the

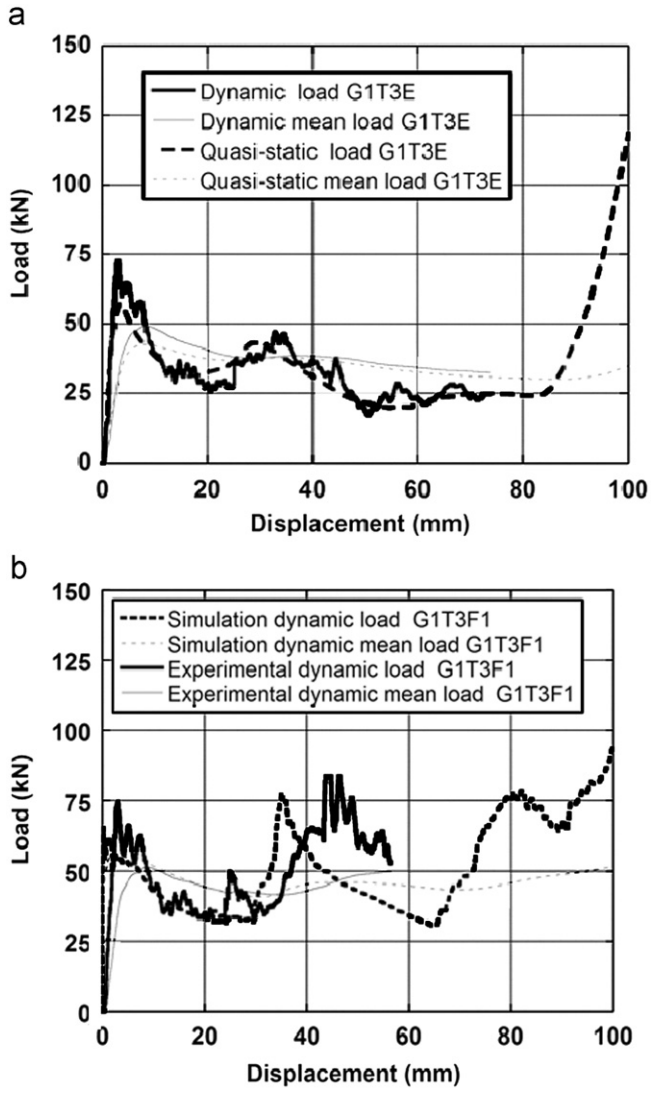

Fig. 13. (a) Dynamic and static load-displacement curve of a 3 mm empty G1 box and (b) simulation and experimental dynamic load-displacement curve of an F1 foam filled 3 mm G1 box.

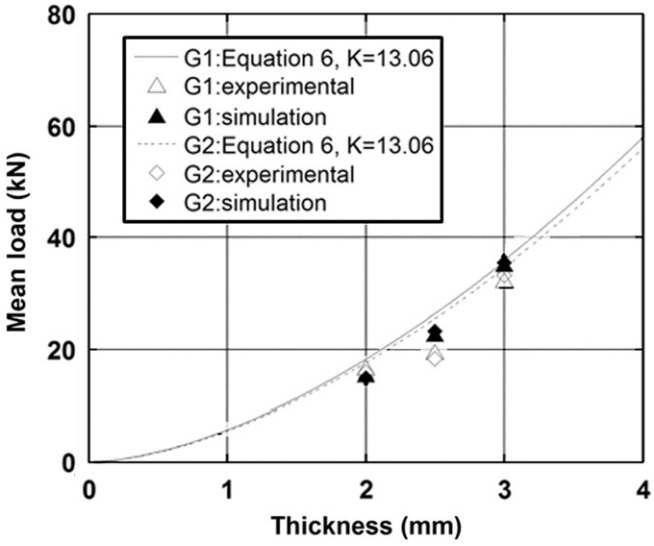

Fig. 14. Fitting experimental and numerical mean load values with Eq. (6).

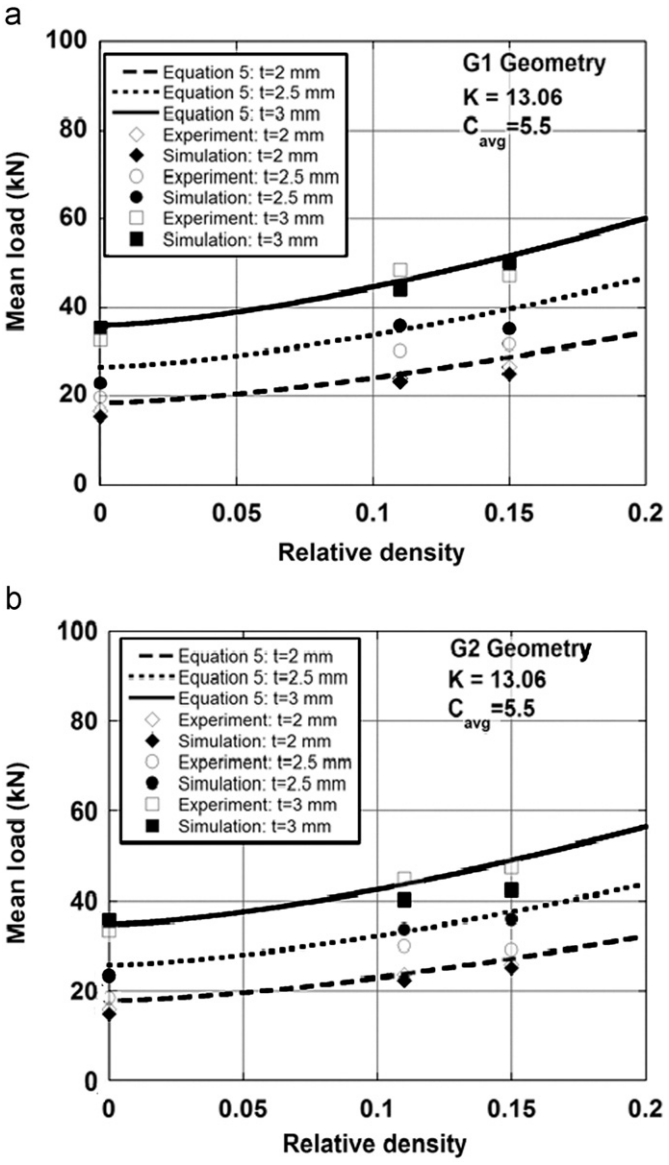

Fig. 15. Mean load vs. foam relative density: (a) G1 and (b) G2 boxes.

impact velocity to 5.5 m s^{-1} has insignificant effects on the load and mean values of empty and partially filled 1050H14 Al crash boxes, agreeing with the well-known strain rate insensitive flow stress behavior of Al.

For full foam filling (filler length is equal to box length), the following equation was previously proposed for the mean crushing load ($P_{m,f}$) [22],

$$P_{m,f} = P_{m,e} + b^2\sigma_f + C_{\text{avg}}\sqrt{\sigma_f\sigma_o}bt \tag{4}$$

where, $P_{m,e}$, b and t are the empty box mean load, width and thickness, respectively. The value of b is taken as the mean of box widths. C_{avg} is a dimensionless constant directly related to the interaction between foam filler and box. The value of C_{avg} increases with increase in deformation and its value at 50% deformation was previously determined 5.5 for fully hydro Al foam filled boxes [22]. In compression testing of partially filled boxes, the foam filler axial deformation starts only after about 60 mm displacement. Therefore, Eq. (4) is rearranged for the partial foam filling by excluding foam filler axial crushing load as

$$P_{m,f} = P_{m,e} + C_{\text{avg}}\sqrt{\sigma_f\sigma_o}bt \tag{5}$$

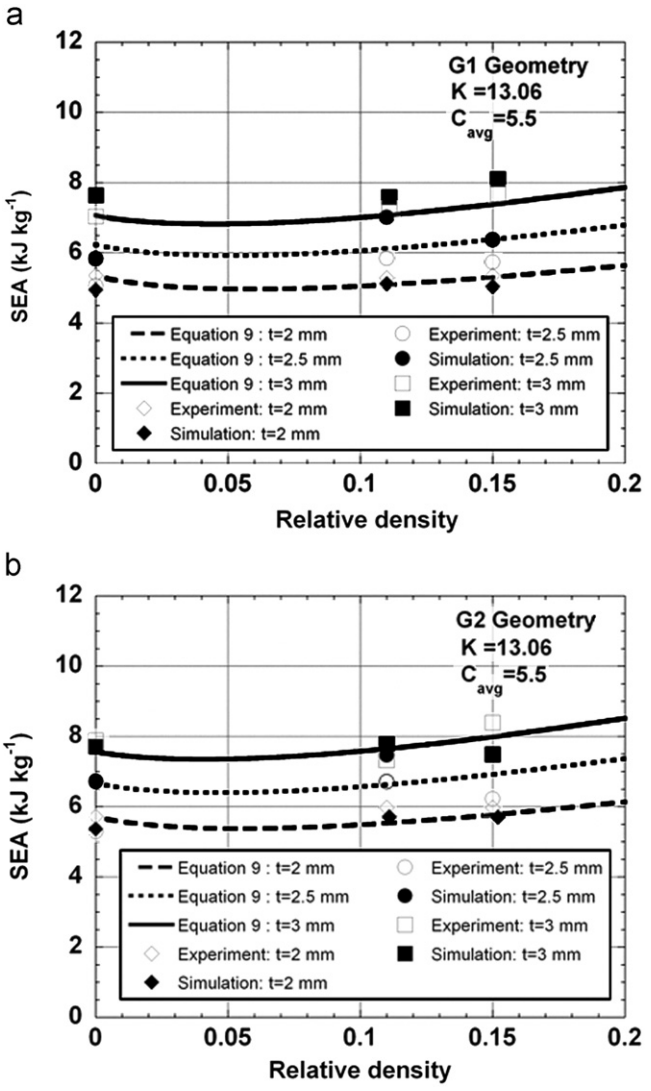

Fig. 16. SEA vs. foam relative density: (a) G1 and (b) G2 boxes.

The empty square box mean load was previously given as [23]

$$P_{m,e} = K\sigma_o b^{1/3} t^{5/3} \tag{6}$$

where K is a dimensionless constant. The value of K was previously proposed to be 13.06 [23]. This value of K shows a good correlation with experimental and simulation mean load values for both G1 and G2 boxes as depicted in Fig. 14. Figs. 15a and b show the variations in experimental and simulation mean load values of G1 and G2 boxes with foam relative density, respectively. In the same graphs, the calculated boxes mean load values using Eq. (5) are also shown. In both boxes, experimental, simulation and calculated mean load values (Eq. (5)) show good correlations with each other (Figs. 15a and b).

The SEA of a crushing column is calculated using the following relation

$$\mathrm{SEA} = \frac{P_m \delta}{m_{\mathrm{total}}} \tag{7}$$

where δ is the effective crash distance, generally taken as 0.75 for empty and filled boxes [16], and m_{total} is the total mass. Since the axial compression of foam filler in filled boxes starts at about 60 mm displacement, the effective crash length of empty and filled boxes is taken to be 0.5L (L: the length of the crash box) for comparison purpose. Therefore, the SEA of empty (SEA_e), partially (SEA_{hf}) and fully (SEA_{ff}) filled boxes are written sequentially as

$$\mathrm{SEA}_e = \frac{(P_{m,e})0.5L}{\rho_{\mathrm{tube}} 4btL} \tag{8}$$

$$\mathrm{SEA}_{hf} = \frac{(P_{m,e} + C_{\mathrm{avg}}\sqrt{\sigma_f \sigma_o}bt)0.5L}{\rho_{\mathrm{tube}} 4btL + \rho_{\mathrm{foam}}(b-t)^2(L/2)} \tag{9}$$

$$\mathrm{SEA}_{ff} = \frac{(P_{m,e} + (b-t)^2\sigma_f + C_{\mathrm{avg}}\sqrt{\sigma_f \sigma_o}bt)0.5L}{\rho_{\mathrm{tube}} 4btL + \rho_{\mathrm{foam}}(b-t)^2 L} \tag{10}$$

where, ρ_{tube} and ρ_{foam} are the box material density and foam filler density, respectively. The SAE values of partially filled G1 and G2 crash boxes calculated using Eq. (9) are shown together with those of experiments and simulations as a function of foam relative density in Figs. 16a and b, respectively. The difference between experimental and simulation and experimental and calculated SEA values are 9.14% and 7.50% on the average, respectively. The calculated SEA values of empty, partially and fully foam filled G1 boxes calculated using Eqs. (8)–(10) are further drawn in Fig. 17 as a function of box wall thickness (between 1 and 3 mm) and foam filler relative density (between 0 and 0.2). The value of C_{avg} of full foam filling in the calculations is taken the same as partial foam filling, 5.5. As is shown in Fig. 17, empty box is energetically more efficient than fully and partially foam filled boxes until about a critical foam relative density, agreeing with the previous studies [16,24]. The critical foam density for efficient foam filling increases slightly as the box wall thickness increases in fully foam filled boxes. The partial foam filling becomes energetically the most efficient at increasing box wall thicknesses at relatively high foam filler densities. It is also noted in Fig. 17 that as the box wall thickness increases, the critical foam density for efficient partial foam filling decreases, opposite to the full foam filling. Fig. 18 shows the simulation and experimental cross-section of a 50 mm compressed F2 foam filled G1 box (without axial compression of foam filler). As shown by arrows, the foam filler resists the inward box wall folding both in numerically and experimentally deformed cross-sections, proving the similar interaction levels in partial and full foam filling.

A simple analysis ($(\mathrm{SEA}_{hf}/\mathrm{SEA}_e) \geq 1$) gives the following relation for the critical foam realtive density (ρ^*_{cr}) for the efficient partial foam filling

$$\rho^*_{cr} \geq \left[\frac{K\sqrt{\sigma_o} b^{1/3}}{8C_{\mathrm{avg}}\sqrt{A}t^{1/3}}\right]^{2/(n-2)} \tag{11}$$

Eq. (11) reveals that the critical foam relative density for efficient partial foam filling is inversely proportional to the box wall thickness, interaction coefficient and foam material strength and directly proportional to box material strength and width. In a previous study [18], the energy absorption of partially foam filled single and double hat steel sections was reported as function of foam filler length. Present results further show that the efficiency of partial foam filling is also a function of box wall thickness and foam filler relative density.

5. Conclusions

The energy absorption behavior of partially Al closed-cell foam filled commercial 1050H14 Al crash boxes in two different sizes and three different thicknesses were determined at quasi-static and dynamic deformation velocities. The foam filler was held in the middle of the crash boxes between the V-grooves intentionally formed on the surfaces of the boxes. A corrugated section initiating the initial box folding was machined near one of the ends of the boxes. The quasi-static and dynamic crushing of

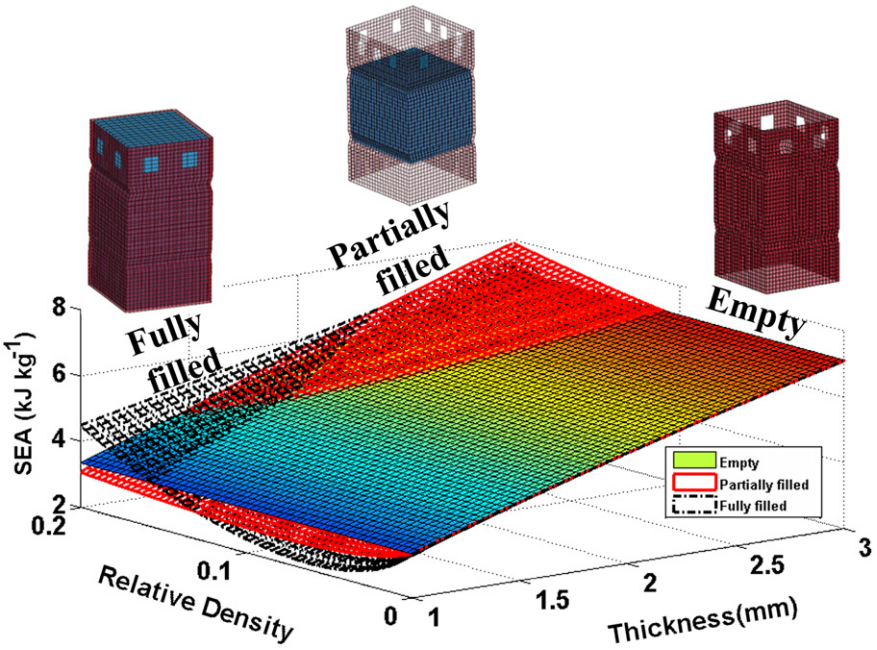

Fig. 17. 3D plots of SEA values of empty, partially filled and fully filled G1 boxes as a function of box wall thickness and foam relative density.

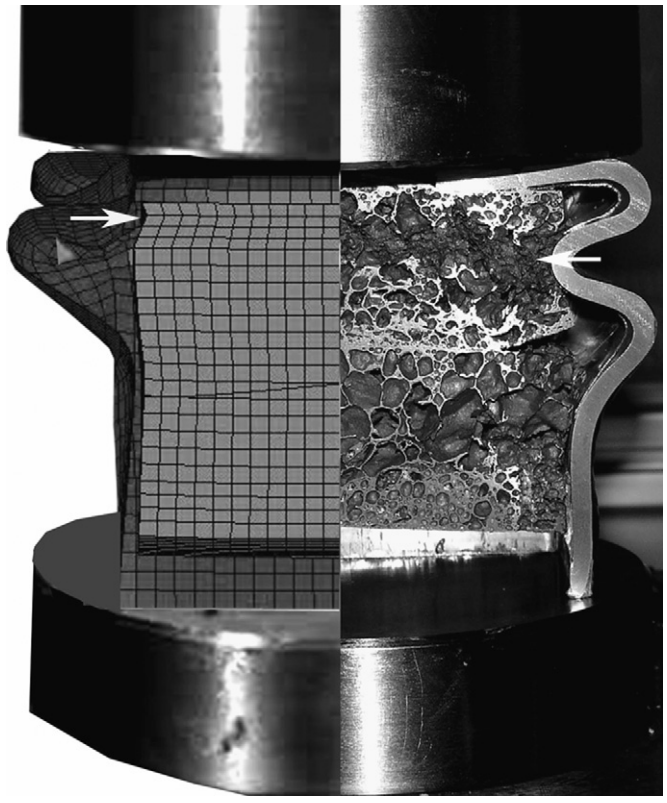

Fig. 18. Simulation and experimental cross-section of a compressed (50 mm) F2 foam filled G1 box.

empty and filled crash boxes were simulated using the LS-DYNA. It was shown both experimentally and numerically that partial foam filling tended to change the deformation mode of empty boxes from a non-sequential to a sequential folding mode. In general, the experimental and simulation results showed similar crushing properties and deformation modes.

In order to assess the efficiency of partial foam filling, the SEA values of empty, partially and fully foam filled boxes were predicted as function of box wall thickness and foam filler relative density. The results showed that empty boxes were energetically more efficient than fully and partially foam filled boxes until about a critical foam relative density, while partial foam filling was energetically the most efficient at increasing box wall thicknesses at relatively high foam filler densities. In contrast with fully foam filling, the critical foam density for efficient partial foam filling decreased with increase in box wall thickness.

Acknowledgement

The authors would like to thank the Scientific and Technical Council of Turkey (TUBITAK) for the grant #106M186.

References

[1] Abramowicz W, Jones N. Dynamic axial crushing of circular tubes. Int J Impact Eng 1984;2(3):263–81.
[2] Abramowicz W, Jones N. Transition from initial global bending to progressive buckling of tubes loaded statically and dynamically. Int J Impact Eng 1997;19(5–6):415–37.
[3] Singace AA, Elsobky H. Further experimental investigation on the eccentricity factor in the progressive crushing of tubes. Int J Solids Struct 1996;33(24):3517–3538.
[4] Langseth M, Hopperstad OS. Local buckling of square thin-walled aluminium extrusions. Thin-Walled Struct 1997;27(1):117–26.
[5] Langseth M, Hopperstad OS, Hanssen AG. Crash behaviour of thin-walled aluminium members. Thin-Walled Struct 1998;32(1–3):127–50.
[6] Han DC, Park SH. Collapse behavior of square thin-walled columns subjected to oblique loads. Thin-Walled Struct 1999;35(3):167–84.
[7] Mamalis AG, Manolakos DE, Ioannidis MB, Kostazos PK, Dimitriou C. Finite element simulation of the axial collapse of metallic thin-walled tubes with octagonal cross-section. Thin-Walled Struct 2003;41(10):891–900.
[8] Liu Y. Crashworthiness design of multi-corner thin-walled columns. Thin-Walled Struct 2008;46(12):1329–37.
[9] Chen W, Wierzbicki T. Relative merits of single-cell, multi-cell and foam-filled thin-walled structures in energy absorption. Thin-Walled Struct 2001;39(4):287–306.
[10] Kim H-S. New extruded multi-cell aluminum profile for maximum crash energy absorption and weight efficiency. Thin-Walled Struct 2002;40(4):311–327.

[11] Seitzberger M, Rammerstorfer F, Degischer H, Gradinger R. Crushing of axially compressed steel tubes filled with aluminium foam. Acta Mech 1997; 125(1):93–105.
[12] Hanssen AG, Langseth M, Hopperstad OS. Static crushing of square aluminium extrusions with aluminium foam filler. Int J Mech Sci 1999; 41(8):967–93.
[13] Santosa S, Wierzbicki T. Effect of an ultralight metal filler on the bending collapse behavior of thin-walled prismatic columns. Int J Mech Sci 1999; 41(8):995–1019.
[14] Song H-W, Fan Z-J, Yu G, Wang Q-C, Tobota A. Partition energy absorption of axially crushed aluminum foam-filled hat sections. Int J Solids Struct 2005;42(9–10):2575–600.
[15] Güden M, Kavi H. Quasi-static axial compression behavior of constraint hexagonal and square-packed empty and aluminum foam-filled aluminum multi-tubes. Thin-Walled Struct 2006;44(7):739–50.
[16] Santosa S, Wierzbicki T. Crash behavior of box columns filled with aluminum honeycomb or foam. Comput Struct 1998;68(4):343–67.
[17] Hanssen AG, Hopperstad OS, Langseth M. Design of aluminium foam-filled crash boxes of square and circular cross-sections. Int J Crash 2001;6(2):177–88.
[18] Wang Q, Fan Z, Song H, Gui L. Experimental and numerical analyses of the axial crushing behaviour of hat sections partially filled with aluminium foam. Int J Crash 2005;10(5):535–43.
[19] ASTM Standard E8/E8M-08. Standart test methods for tension testing of metallic materials. In: ASTM international, PA: West Conshohocken; 2003.
[20] Williams BW, Oliveira DA, Simha CHM, Worswick MJ, Mayer R. Crashworthiness of straight section hydroformed aluminium tubes. Int J Impact Eng 2007 34(8):1451–1464.
[21] Santosa SP, Wierzbicki T, Hanssen AG, Langseth M. Experimental and numerical studies of foam-filled sections. Int J Impact Eng 2000;24(5): 509–534.
[22] Hanssen AG, Langseth M, Hopperstad OS. Static and dynamic crushing of square aluminium extrusions with aluminium foam filler. Int J Impact Eng 2000;24(4):347–83.
[23] Abramowicz W, Jones N. Dynamic progressive buckling of circular and square tubes. Int J Impact Eng 1986;4(4):243–70.
[24] Kavi H, Toksoy AK, Guden M. Predicting energy absorption in a foam-filled thin-walled aluminum tube based on experimentally determined strengthening coefficient. Mater Des 2006;27(4):263–9.